Inorganic Chemistry

Article

pubs.acs.org/IC

Cu(I) Complexes of Pincer Pyridine-Based N-Heterocyclic Carbenes with Small Wingtip Substituents: Synthesis and Structural and Spectroscopic Studies

Doaa Domyati, Sydney L. Hope, Reza Latifi, Micah D. Hearns, and Laleh Tahsini*

Department of Chemistry, Oklahoma State University, Stillwater, Oklahoma 74078, United States

Supporting Information

ABSTRACT: Six new Cu(I) complexes with pincer N-heterocyclic carbene (NHC) ligands of the type 2,6-bis(3-alkylimidazol-2-ylidene)pyridine, I(R)^{CNC}, and 2,6-bis(3-alkylimidazol-2-ylidene)methylpyridine, I(R)$^{C\wedge N\wedge C}$, where R = Me, Et, and ^{i}Pr have been synthesized using Cu precursors and bis(imidazolium) salts. All of these compounds, namely, $[Cu_2(IMe^{CNC})_2](PF_6)_2$, **1**; $[Cu_2(IEt^{CNC})_2](PF_6)_2$, **2**; $[Cu_2(I^{i}Pr^{CNC})_2](PF_6)_2$, **3**; $[Cu(IMe^{C\wedge N\wedge C})](PF_6)$, **4**; $[Cu(IEt^{C\wedge N\wedge C})](PF_6)$, **5**; and $[Cu(I^{i}Pr^{C\wedge N\wedge C})](PF_6)$, **6**, have been characterized by ^{1}H and ^{13}C NMR spectroscopies, elemental analysis, solution conductivity, and electrochemical studies. Single crystal X-ray structures were obtained for all complexes except **1**. The crystallographic data reveal a binuclear structure containing two Cu atoms at a close distance, 2.622−2.811 Å for all the complexes except **5**, which shows a unique mononuclear structure. Spatial syn arrangement of ethyl groups and extensive $\pi-\pi$ stacking in the solid state accounts for the mononuclear structure of complex **5**. A pseudolinear coordination geometry about metal centers consisting of two Cu−carbene bonds, as well as weak Cu−pyridine interactions, exist among all the complexes independent of their ligand. Solution-state conductivity data reveal a dominant 1:2 electrolyte behavior for **1**−**3** but 1:1 electrolyte for **4**−**6**, consistent with the sustainable binuclear structure in solutions of Cu(I)−I(R)^{CNC} complexes. Cyclic voltammetry and differential pulse voltammetry studies reveal an irreversible and two quasi-reversible peaks for the one-electron oxidation of solvent-bound and solvent-free binuclear and mononuclear Cu-NHC species in complexes **1**−**3**. In contrast, the reversible Cu(II)/Cu(I) couples of **4**−**6** at potentials close to that of complexes with tripodal polydentate NHC scaffolds indicate the electronic and structural flexibility of I(R)$^{C\wedge N\wedge C}$ ligands to accommodate both Cu(I) and Cu(II) ions.

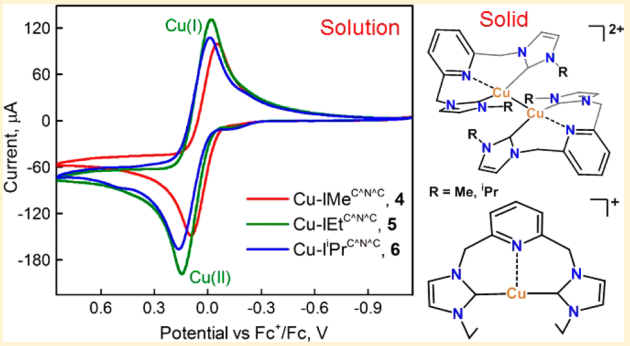

INTRODUCTION

The first isolation of a thermally stable carbene[1] and the first catalytic application of Pd−NHC complexes in Heck coupling reactions[2] have blossomed into tremendous growth in the field of organometallic synthesis and catalysis over the past two decades. One of the most valuable characteristics of NHC ligands for catalytic applications is their strong σ-donating property, which allows the formation of strong bonds to different transition metals, increasing the stability of the complexes. While a large number of NHC complexes of precious metals have been prepared and used in various organic transformations,[3−5] there is currently a growing interest in developing the complexes of less expensive, non-noble metals, specifically copper.[6−8] Over the past decade, numerous Cu−NHC systems have been developed mainly with mono-NHC ligands in neutral [Cu(NHC)X] (X = halide, acetate, hydride, etc.)[9−14] or cationic [Cu(NHC)L]X (L = NHC or phosphines; X = PF_6 or BF_4)[15−18] complexes. Some of the complexes have been utilized as catalysts in hydrosilylation,[19,20] click chemistry,[21] or alkene boration[22−24] and have been reviewed.[6] Despite the enhanced stability of complexes with bis- or poly-NHC ligands due to the chelate effect, the examples of structurally characterized Cu−bis(NHC) systems are very limited. Incorporating noncarbene donors (N, O, and S) in bis- and tris-NHC ligands has created numerous polydentate ligands[25] that in many cases result in multinuclear copper complexes. Structural parameters such as the size of linker groups, the location of noncarbene donors, the overall flexibility of NHC ligands, the steric bulk of wingtip groups, and the reaction conditions determine the coordination mode of Cu with polydentate NHC ligands. For example, the first Cu−poly(NHC) complexes with tris-[2-(3-alkylmethylimidazol-1-ylidene)ethyl]ethane (TIME^{R}), a tris(NHC) ligand, provided different copper nuclearity depending on the reaction conditions and the substituents on the imidazolium rings. A trinuclear complex was obtained via transmetalation using Ag_2O, whereas a binuclear structure was generated when a strong base was used for deprotonation and $[Cu(CH_3CN)_4]^{+}$ as the copper source.[26] When the C-anchor was replaced by an

Received: July 13, 2016

DOI: 10.1021/acs.inorgchem.6b01646
Inorg. Chem. XXXX, XXX, XXX−XXX

Scheme 1. Synthesis of Cu−NHC Complexes

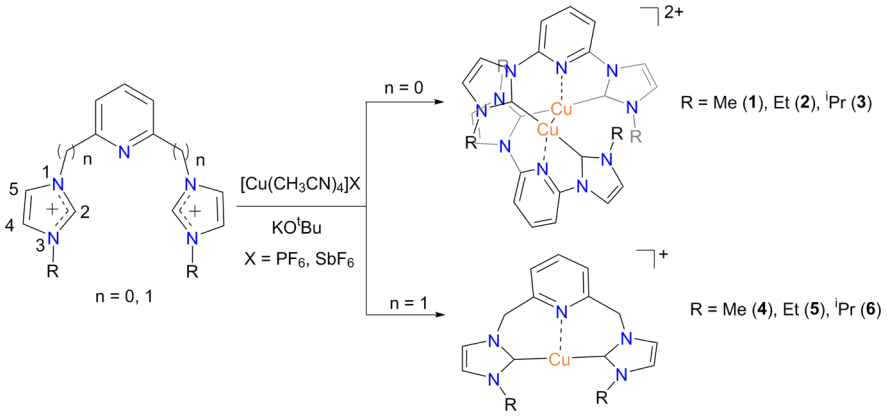

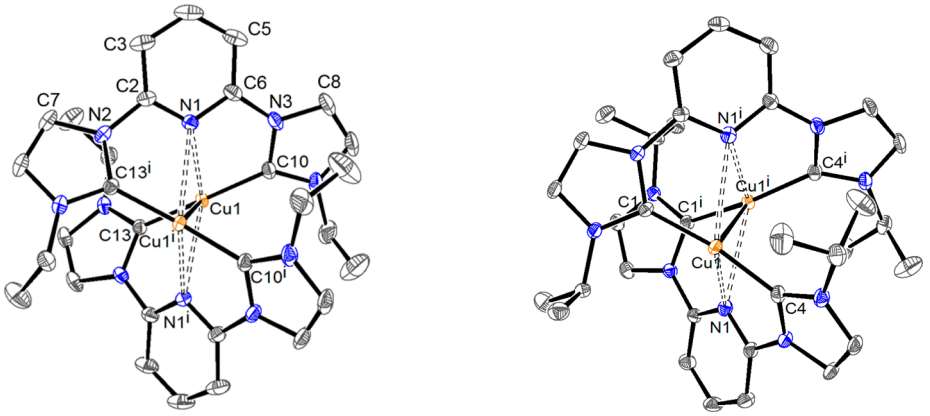

Figure 1. ORTEP diagrams of $[Cu_2(IEt^{CNC})_2](PF_6)_2$, **2** (left), and $[Cu_2(I^iPr^{CNC})_2](SbF_6)_2$, **3**-$SbF_6$ (right). Anions and hydrogens are omitted for clarity. Ellipsoids are shown at the 50% probability level.

N-anchor in the TIME^R structure with bulky wingtip groups (R = *tert*-butyl and benzyl), a mononuclear Cu−tris(NHC) complex was prepared. The same ligand afforded a trinuclear copper complex when the small methyl groups were substituted on the imidazolium rings.[27]

The copper complexes with pincer COC ligands are a class of Cu−bis(NHC) complexes in which two NHC units are linked via an O-donor group such as 1,2-diethoxybenzene[28] or 2-phenylpropane-2-oxide.[29] The first ligand bearing a more flexible linker and the bulky 1-naphthylmethylene groups provided a mononuclear copper complex, whereas the second ligand with the alkoxide linker and *tert*-butyl substituents resulted in a binuclear structure. Each oxygen atom in the later complex coordinates to two copper centers along with the two NHC units supporting a square-planar geometry around both metals.[29]

The copper compounds with nonpincer NHC ligands linked via an alkyl group comprise a second class of Cu−bis(NHC) complexes, forming diverse metal clusters in solid state. A CH_2-bridged bis(imidazolium) salt bearing *t*-butyl wingtips formed a coordination polymer.[30] The same carbene backbone with pyridyl wingtips supported a binuclear Cu(I) complex in a reaction of imidazolium salt with Cu powder in air, but a trinuclear complex formed in a transmetalation process.[31] A slightly different carbene, hydroxymethyl-functionalized CH_2-bridged analogue bearing methyl groups, afforded only a binuclear Cu(I) complex after transmetalation via Ag_2O.[32] The more flexible ethylene-bridged NHC ligand with vinyl or propylene substituents, however, formed different coordination modes of Cu(I) including bi-, tetra-, and polynuclear in the presence of different equivalents of KO^{t}Bu.[33]

Metal clusters have governed potential application in material science and catalysis.[34−36] While the presence of multiple metal centers creates unique magnetic and electronic properties, it makes it difficult as well to develop molecular-level understanding of their chemistry via common analytical techniques. In this context, we are particularly interested in pyridine-based pincer NHC ligands with small wingtip groups due to their low flexibility, which can render the formation of copper complexes of lower nuclearity. It is also hypothesized that the presence of both hard (N) and soft (C) atom donors in the structure of such ligands can support the formation of low- and high-valent metal ions. There are only three examples of crystallographically characterized copper complexes with pyridine-linked bis(NHC) ligands in literature.[37−39] To the best of our knowledge, however, no report exists of the copper−NHC complexes where two NHC groups are bridged by a pyridylalkyl linker. We describe herein, the one-pot synthesis and characterization of six new Cu(I)−bis(NHC) complexes with pyridine and pyridylmethyl linkers.

RESULTS AND DISCUSSION

Synthesis of Cu−NHC Complexes 1−6. Cu−NHC complexes **1−6** were obtained from the reaction of $[Cu(CH_3CN)_4]PF_6$ or $[Cu(CH_3CN)_4]SbF_6$ and an in situ generated NHC at room temperature in the absence of air and moisture. The NHC ligands were generated by

DOI: 10.1021/acs.inorgchem.6b01646
Inorg. Chem. XXXX, XXX, XXX−XXX

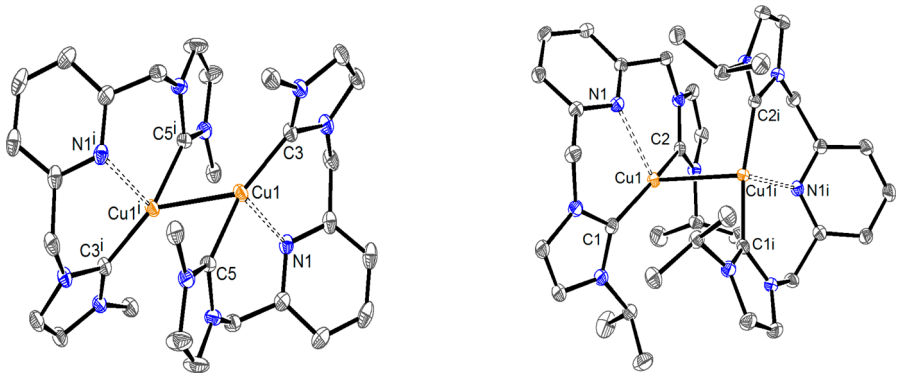

Figure 2. ORTEP diagrams of $[Cu(IMe^{C\wedge N\wedge C})](PF_6)$, **4** (left), and $[Cu(I^iPr^{C\wedge N\wedge C})](PF_6)$, **6** (right). Anions and hydrogens are omitted for clarity. Ellipsoids are shown at the 50% probability level.

deprotonating imidazolium salts with KO^{t}Bu, and reaction with copper precursors afforded yellow solids in very good yields (Scheme 1). The imidazolium salts were also prepared by quaternization of *N*-alkylimidazole derivatives with 2,6-dibromopyridine or 2,6-dibromomethylpyridine. Complexes **1**−**3** were stable in air and could be stored as solids in air for weeks or in solution for days. However, solutions of **4**−**6** oxidized in air in less than 5 h to form green Cu(II) species. Single crystal X-ray structures of all copper complexes were determined except **1**. Among all the proton signals of imidazolium rings and pyridine linkers that are upfield shifted in complexes compared to the imidazolium precursors, H^4 and H^5 proton signals of imidazolium have the greatest shifts (∼0.8 ppm). The H^2 proton signal of the imidazolium rings has also disappeared in the ^{1}H NMR spectra of copper complexes **4** and **5** as compared to the corresponding imidazolium salts. The H^2 protons do not appear in the ^{1}H NMR spectra of the rest of the imidazolium salts, due to a rapid exchange with residual water in deuterated methanol. The ^{13}C NMR spectra of the complexes exhibit resonance signals at 178−182 ppm due to the carbenic carbon atoms, consistent with the reported chemical shifts of other Cu−NHC complexes.[10,16,26]

X-ray Crystallography of Cu−NHC Complexes 2−6. Single crystals of complexes **2**−**6** were obtained by slow diffusion of diethyl ether into an acetonitrile solution of copper complexes at room temperature. Crystallographic data collection parameters are summarized in Table S1 with selected distances and angles in Table S2.

With no CH_2 groups between the NHC and py groups, each Cu center in **2** and **3** is bound to NHC units from two different ligands, forming cationic, dimeric compounds containing two-coordinate Cu(I) centers (Figure 1). The C−Cu−C bond angles are slightly bent with values of 166.45(6)° and 166.56(8)° for **2** and **3**-SbF_6, respectively. The NHC rings form dihedral angles with the pyridyl bridges of 14.49(2)° and 28.0(2)° in **2** and 23.88(3)° and 23.34(3)° in **3**. The average Cu−C_{NHC} bond distances are in accordance with the reported values in other Cu(I)−NHC complexes[32] including $[Cu_2(IEt^{CNC})_2](BF_4)_2$,[39] $[Cu_2(I^tBu^{CNC})_2](PF_6)_2$,[37] and $[Cu_2(I^nBu^{CNC})_2](PF_6)_2$.[38] The Cu···$N_{py}$ distances are consistent with other ancillary pyridine donors.[37,38,40] The Cu···Cu distances of 2.805(7) Å in **2** and 2.811(3) Å in **3** are close to the sum of the van der Waals radii for two copper atoms (2.80 Å), are cuprophilic interactions, and are shorter than those reported for $[Cu_2(IEt^{CNC})_2](BF_4)_2$, 2.956(1) Å, and $[Cu_2(I^tBu^{CNC})_2](PF_6)_2$, 3.206(5) Å.[37,39] The effect of counteranion on metallophilic interactions has been discussed in a series of Au(I)−carbene complexes, $[Au\{C(OMe)NHMe\}_2]X$ (X = $CF_3SO_3^-$, ClO_4^-, PF_6^-, $CF_3CO_2^-$, and I^-),[41] in which the aurophilic distances were affected by anion steric hindrance and hydrogen bonding.

The difference (0.150 Å) between the Cu···Cu distances in **2**-PF_6 and **2**-BF_4 cannot be fully explained by hydrogen bonding. Shown in Figure S1 are the long-range interactions between fluorines and alkenic hydrogens on the imidazoline/pyridyl rings in both complexes, **2**-PF_6 and **2**-BF_4. Despite the greater number of F···H interactions in **2**-PF_6, a shorter bond was found between copper ions. These complexes crystallize in different space groups with **2**-BF_4 crystallizing in trigonal *R*32 and **2**-PF_6 in monoclinic *P*2/*n*. The chirality of **2**-BF_4 is retained in solution as evident from its nonequivalent N-ethyl CH_2 protons in the ^{1}H NMR spectrum.[39] In contrast, **2**-PF_6 reveals only one resonance at 3.69 ppm likely due to a dynamic exchange process (Figure S2).

In the crystal structures of complexes **4**−**6**, each copper is bound to two NHC moieties from the same pincer ligand, in contrast to Cu(I)−I(R)^{CNC} **2** and **3** above. The structure of $[Cu(IMe^{C\wedge N\wedge C})](PF_6)$, **4** (Figure 2), has two Cu(I) centers at a Cu···Cu distance of 2.622(3) Å and an average Cu−C_{NHC} distance of 1.941(2) Å, longer than that of the rest of the compounds in this study, but in the range of other Cu−NHC complexes.[29,42,43] The Cu···N_{py} and Cu···Cu distances in **4** are substantially shorter than those in **2** and **3**, and the cuprophilic interaction in **4** is the shortest interaction between two Cu(I) ions in this study.

The structure of $[Cu(I^iPr^{C\wedge N\wedge C})](PF_6)$, **6** (Figure 2), has Cu−C_{NHC} average bond lengths of 1.910(1) and 1.919(2) Å, and an elongated cuprophilic Cu···Cu distance at 2.735(3) Å compared to **4**. The stereochemistries of the two Cu−NHC units in **4** and **6** are distinct as indicated by the dihedral angle (θ) between {N_{py}−Cu−Cu} planes (Scheme 2). The Cu−N_{py}

Scheme 2. Calculation of Dihedral Angle between Two N_{py}CuCu′ Planes in Complexes 4 and 6

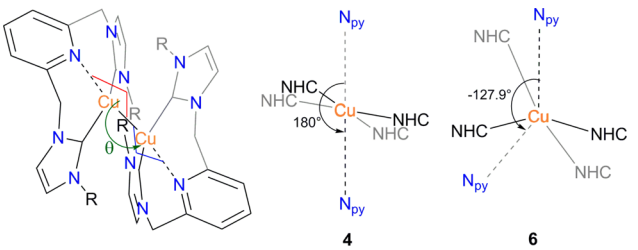

DOI: 10.1021/acs.inorgchem.6b01646
Inorg. Chem. XXXX, XXX, XXX−XXX

bonds in **4** have antiparallel alignment and a dihedral value of 180° due to an antiperiplanar conformation. In **6**, however, the nonparallel orientation of the Cu−N_{py} bonds with respect to one another results in a dihedral angle of −127.92° in an anticlinal conformation. The distinct arrangement of mononuclear Cu−NHC motifs in these complexes is likely influenced by the imidazole wingtip substituent steric hindrance.

Unlike complexes **2**, **3**, **4**, and **6**, **5** has a mononuclear structure for $[Cu(IEt^{C\wedge N\wedge C})](PF_6)$, **5** (Figure 3). The average

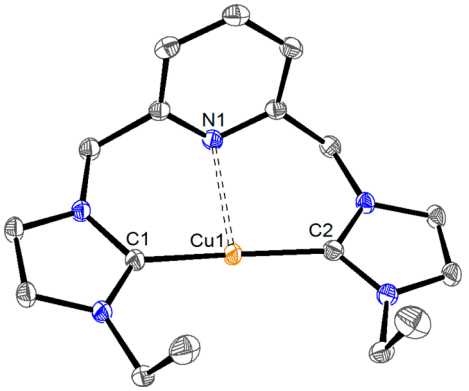

Figure 3. ORTEP diagram of $[Cu(IEt^{C\wedge N\wedge C})](PF_6)$, **5**. Anions are omitted for clarity. Ellipsoids are shown at the 50% probability level.

Cu−C_{NHC} bond distance of 1.910(1) Å is similar to those determined for the binuclear complexes, but the Cu···Cu distance of 3.239(2) Å is too long for a metallophilic interaction. Figure S3 displays $\pi-\pi$ stacking interactions in **5** between the facial imidazoline rings of two mononuclear Cu−bis(NHC) at a 3.540(1) Å and separate π-stacking interaction of pyridine rings at 3.730(3) Å. Interestingly, **5** is the only complex in this study that presents π-stacked ring systems in the solid state. In general, the Cu−$I(R)^{C\wedge N\wedge C}$ complexes have more diverse solid-state structures, unlike the Cu−$I(R)^{CNC}$ complexes, which are similar to one another. The low steric hindrance of Me groups in Cu−$IMe^{C\wedge N\wedge C}$ allows a symmetric antiparallel arrangement of two $[Cu(IMe^{C\wedge N\wedge C})]^+$ units at the shortest Cu···Cu distance in this study. The bulkier ^{i}Pr groups, in contrast, enforce a nonparallel orientation of two monomers in an anticlinal conformer to retain the cuprophilic interaction. In **5**, a close Cu(I) contact is disfavored due to the steric pressure of Et groups in a syn conformation; however, the $\pi-\pi$ stacking interactions between rings may account for the monomeric structure.

Solution State Conductivity of Cu−NHC Complexes. The solution conductivities of the Cu−$I(R)^{CNC}$ and Cu−$I(R)^{C\wedge N\wedge C}$ complexes were measured in acetonitrile with $^nBu_4NPF_6$ as a reference. The Onsager plots[44,45] for all complexes and the 1:1 electrolyte control are shown in Figure 4. Complexes **4**−**6** exhibit 1:1 electrolyte conductivity indicating the absence of metallophilic interactions in solution. Complexes **1**−**3** show greater conductivities than their analogues with $I(R)^{C\wedge N\wedge C}$ ligands (**4**−**6**), consistent with 50% more ions in solution. The calculated molar conductivity (Λ_M) values of 334, 333, and 313 at 1 mM concentrations of **1**, **2**, and **3**, respectively, fall within the expected Λ_M range for a 2:1 electrolyte in acetonitrile.[44]

The data in Figure 4 indicate that the dimeric copper complexes **1**−**3** remain so in solution, whereas the unsupported

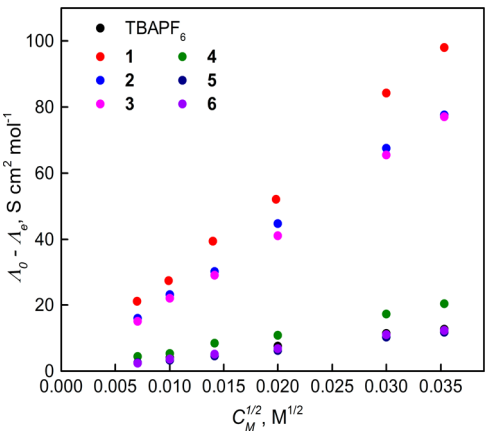

Figure 4. Solution conductivity studies of complexes **1**−**6** and $^nBu_4PF_6$ in CH_3CN.

Cu···Cu interactions in **4**−**6** are disrupted. Therefore, the metallophilic interactions in these complexes do not persist in solution. This clean switch of the electrolyte behavior between the two classes is strongly influenced by the relative flexibility of $I(R)^{C\wedge N\wedge C}$ ligands that facilitates the loss of Cu···Cu interactions in **4**−**6**. Furthermore, the viability of the binuclear complexes **1**−**3** in solution is supported by their unique coordination environment where each Cu(I) is bound to both of the NHC molecules. Indeed, it has been shown that the conformational fluxionality in solution leads to the loss of cuprophilic interaction in $[Cu_2(IEt^{CNC})_2](BF_4)_2$ complex.[39]

Electrochemical Studies of Cu−NHC Complexes. The cyclic and differential pulse voltammograms of **1**−**3** exhibit three redox peaks of different heights within the accessible potential window (Figure 5). The $IMe^{CNC}\cdot 2HPF_6$ control presents no reduction/oxidation features under the same conditions. Interestingly, the first and second oxidation peaks (A and B in Figure 5b) were absent from the CV of $[Cu_2(IEt^{CNC})_2](BArF)_2$ in CH_2Cl_2; however, the peak B reappeared when a small amount of CH_3CN (0.5 mL) was introduced into the solution. The significant increase in current in a mixture of CH_3CN and CH_2Cl_2 (1:7) is attributed to the improved solubility of Cu−$I(R)^{CNC}$ complexes in polar solvents. The peak current intensity due to the three oxidation events (A, B, and C) compares well to the peak current of $[Cp_2Fe]$ under similar conditions, consistent with one-electron oxidation of all Cu^I−$I(R)^{CNC}$ species in solution (Figure S4). These observations are consistent with multiple speciation of complexes **1**−**3** in acetonitrile as a coordinating solvent to form solvent-bound Cu−NHC species, possibly mono- and binuclear complexes, as shown in Scheme 3. In the absence of direct structural evidence, the first oxidation peak (A) can be assigned to a solvent-bound mononuclear couple, for example, $[LCu^IS]^+/[LCu^{II}S]^{2+}$, due to a similar potential to that of mononuclear Cu−$I(R)^{C\wedge N\wedge C}$ **4**−**6** (vide infra). The amount of the $[LCu^IS]^+$ was estimated to be around 15% of that of Cu-IEt^{CNC}, assuming that the transfer and diffusion coefficients in the irreversible Delahay equation[46,47] are similar for all the Cu(I)−IEt^{CNC} species (Figure S5 and eq S1). The predominance of the binuclear species in solutions of Cu−$I(R)^{CNC}$ complexes was demonstrated above in the conductivity studies.

The CV experiments were also carried out in varying potential window sizes to identify which reduction and oxidation peaks are associated with one another (Figure S6). In **1**, the first oxidation peak at −0.071 V (vs Fc^+/Fc) and the

DOI: 10.1021/acs.inorgchem.6b01646
Inorg. Chem. XXXX, XXX, XXX−XXX

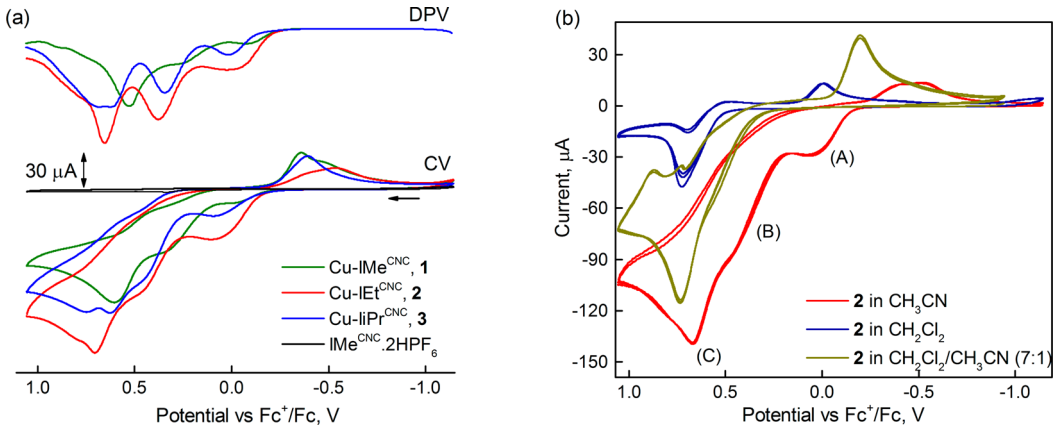

Figure 5. (a) Cyclic voltammograms (CV) and differential pulse voltammograms (DPV) of **1**–**3** (5.0 mM) reported vs Fc^+/Fc in deaerated acetonitrile/$^nBu_4PF_6$ (0.1M) at 0.1 V s^{-1} scan rate. The arrow shows the scan direction starting at −0.143 V. (b) Cyclic voltammograms of Cu–IEt^{CNC} (4.6 mM) in acetonitrile, dichloromethane, and their mixture. Three cycles of all CVs are shown.

Scheme 3. Speciation and Electron Transfer in Cu–I(R)^{CNC} Complexes

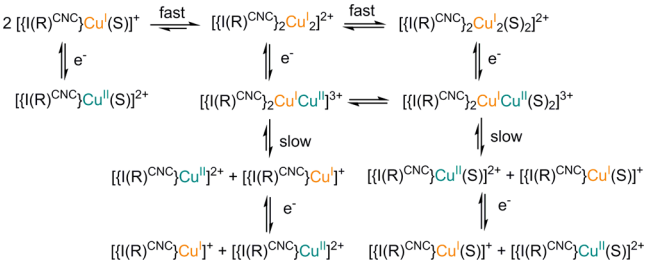

corresponding reduction at −0.524 V are attributed to the mononuclear $[LCu^IS]^+/[LCu^{II}S]^{2+}$ couple. The cyclic voltammograms at higher scan rates revealed an increase in the peak current and a shift in the reduction potential of this couple to more negative values, indicative of a quasi-reversible system (Figure S7). The next two oxidation peaks (B and C) in the CV of **2** are assigned to the one-electron oxidation of solvent-bound $[L_2Cu_2^IS_x]^{2+}$ and solvent-free $[L_2Cu^I_2]^{2+}$ binuclear complexes, respectively, again shown in Scheme 3. These features happen at 0.257 and 0.529 V (vs Fc^+/Fc) for the Cu–IMe^{CNC} complex, but at slightly higher potentials, 0.375 and 0.651 V for **2** and 0.341 and 0.619 V for **3**. The small reduction peak of the $[L_2Cu^{II}Cu^I]^{3+}/[L_2Cu^I_2]^{2+}$ couple in the reverse scan and barely noticeable return peak of the $[L_2Cu^{II}Cu^IS_x]^{3+}/[L_2Cu_2^IS_x]^{2+}$ support the electron-transfer followed by a chemical step. The presence of a new reduction peak nearby the $[LCu^IS]^+/[LCu^{II}S]^{2+}$ couple as well as the increase in the cathodic peak current of $[LCu^IS]^+$ species at large potential windows are consistent with splitting the oxidized binuclear complexes into monomers (Figure S6). This process, however, is not a completely irreversible transformation, since no significant change occurs in the overall shape and intensity of the oxidation or reduction peaks over multiple scans (Figure S8). The electron transfer, chemical reaction, and electron transfer (ECE) mechanism for the solvent-bound and solvent-free binuclear Cu–I(R)^{CNC} complexes was also confirmed by comparing the cyclic voltammograms of small and large potential window sizes at two different scan rates, 0.05 vs 1.0 V s^{-1} (Figure S9). The increase in the cathodic peak current of $[LCu^IS]^+/[LCu^{II}S]^{2+}$ couple due to breaking up the binuclear species in a large potential window is greater with a faster potential sweep. This phenomenon indicates a drastic increase in the equilibrium constant of dissociation process by the subsequent fast electron transfer at 1.0 V s^{-1} scan rate. The three oxidation peaks in the CV of complex **2** were observed regardless of the scan rate indicating a very fast equilibrium between the solvent-bound/solvent-free mononuclear and binuclear species in solution (Figure S10). Shown in Scheme 3 is a mechanism for the speciation and the electron transfer processes of Cu–I(R)^{CNC} complexes based on the electrochemical and solution conductivity data.

Interestingly, the cyclic voltammograms of the monomeric $[Cu(I(R)^{C^N^C})](PF_6)$ complexes reveal an entirely different behavior compared to $[Cu_2(I(R)^{CNC})_2]^{2+}$ systems. The results are summarized in Table 1. As shown in Figure 6 and Table 1, a single reversible peak was observed due to the Cu(II)/Cu(I) couple with $E_{1/2}$ values at 0.021, 0.063, and 0.077 V (vs Fc^+/Fc) for **4**, **5**, and **6**, respectively. Plotting current plot versus the square root of scan rate (Randles–Sevcik equation) (Figure S11) confirms the reversibility of the Cu(II)/Cu(I) couple, indicating that the $I(R)^{C^N^C}$ ligands have sufficient structural and electronic flexibility to accommodate both Cu(I) and Cu(II) oxidation states. To the best of our knowledge, this is the first time that a reversible Cu(II)/Cu(I) couple is demonstrated with a nonmacrocyclic or polydentate NHC system. A reversible Cu(II)/Cu(I) couple was demonstrated in a tripodal poly(NHC) system, $TIMEN^{t\text{-}Bu}$, with $E_{1/2}$ at +0.110 V (vs Fc^+/Fc).[27] The presence of only one redox couple in the cyclic voltammograms of **4**–**6** also indicates the loss of

Table 1. Cyclic Voltammetry Data for Complexes 4–6 and Comparison to Literature Complexes

complex	$E_{1/2}$[a] (V)	ΔE_p (V) = $E_{pc} - E_{pa}$	ref
$[Cu(IMe^{C^N^C})](PF_6)$, **4**	0.021	0.149	this work
$[Cu(IEt^{C^N^C})](PF_6)$, **5**	0.063	0.166	this work
$[Cu(I^iPr^{C^N^C})](PF_6)$, **6**	0.077	0.176	this work
Fc	0	0.137	this work
$[(TIMEN^{t\text{-}Bu})Cu](PF_6)$	0.110[b]	0.066[b]	27

[a]Recorded in CH_3CN containing 5 mM $[Cu_2(I(R)^{C^N^C})_2](PF_6)_2$ or Cp_2Fe (Fc) at 0.1 V s^{-1} scan rate vs Fc^+/Fc, $E_{1/2} = (E_{pc} + E_{pa})/2$, where E_{pc} and E_{pa} are cathodic and anodic peak potentials, respectively. [b]Recorded in CH_3CN containing 0.1 M $^nBu_4NClO_4$ as electrolyte vs Fc^+/Fc and at 0.3 V s^{-1} scan rate.

DOI: 10.1021/acs.inorgchem.6b01646
Inorg. Chem. XXXX, XXX, XXX–XXX

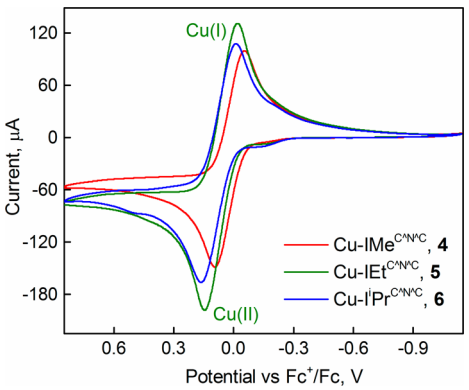

Figure 6. Cyclic voltammograms of **4**–**6** (5.0 mM) reported vs Fc^+/Fc in deaerated $CH_3CN/^nBu_4NPF_6$ (0.1M) indicating one-electron redox process. The scan rate was 0.1 V s^{-1}.

cuprophilic interactions and the dominance of monomeric $[Cu(I(R)^{C^N^C})]^+$ species in solution, consistent with the conductivity data. Complexes **4**–**6** are similar to $[Cp_2Fe]$ based on their $E_{1/2}$ values (Table 1). The observed increase in the Cu(II)/Cu(I) half-wave potential of Cu–$I(R)^{C^N^C}$ complexes from methyl to ethyl and isopropyl substituents is consistent with increase in the steric hindrance of the NHC ligands. The presence of bulky groups disfavor the expansion of coordination number in Cu(II) complexes by inhibiting solvent binding. A similar trend was observed between the ligands steric effects and Cu(II)/Cu(I) redox potential in a series of Cu–Phen complexes.[48−50] According to the data in Table 1, smaller wingtip substituents on NHC ligands would favor high oxidation states of metals.

EXPERIMENTAL SECTION

General Procedure. Imidazolium salt and Cu(I) complex syntheses were performed using standard Schlenk techniques or in an MBraun glovebox under Ar atmosphere. The solvents used for the syntheses and analytical studies of copper complexes were purified and distilled under N_2 atmosphere before being stored over activated molecular sieves (4 Å) in the glovebox. Tetrahydrofuran and diethyl ether were purified by refluxing over Na/benzophenone under a N_2 atmosphere and distilled. Acetonitrile and hexane were distilled from CaH_2 under N_2. Anhydrous 1,4-dioxane was obtained from Sigma-Aldrich and used as received. Potassium *tert*-butoxide (97%) was obtained from Sigma-Aldrich and crystallized from THF in the glovebox. Imidazole derivatives, 2,6-dibromopyridine, and 2,6-dibromomethylpyridine were obtained from TCI America and used without further purification. NMR samples were prepared under Ar in deuterated solvents, MeOD or CD_3CN, containing 0.05% TMS as internal standard. $[Cu(CH_3CN)_4](PF_6)$ was obtained from Sigma-Aldrich, and $[Cu(CH_3CN)_4]SbF_6$ was synthesized according to a published procedure.[51] $[Cu(CH_3CN)_4]BArF$ (BArF = tetrakis-(pentafluorophenyl)borate) was prepared from the reaction of $[Cu(CH_3CN)_4](PF_6)$ and KBArF in acetonitrile. The imidazolium salts, $I(R)^{CNC}\cdot 2HBr$ and $I(R)^{C^N^C}\cdot 2HBr$ (R = Me, Et and ^{i}Pr), were synthesized by some modification of the published procedures (see Supporting Information).[52,53] Tetrabutylammonium hexafluorophosphate ($^nBu_4NPF_6$) for electrochemical studies was doubly recrystallized from dichloromethane and diethyl ether. NMR spectra were measured using a 400 MHz Bruker Avance III spectrometer. Chemical shifts (δ) for ^1H and ^{13}C NMR spectra were referenced to the resonance of TMS as an internal reference or the residual protio solvent. Conductivity studies were performed at room temperature using a Fisher Scientific traceable portable conductivity meter (model number 09-326-2). Elemental analyses were performed by Atlantic Microlabs, Inc. (Norcross, Georgia).

Copper Complex Syntheses. *$[Cu_2(IMe^{CNC})_2](PF_6)_2$*, ***1***. A portion of $IMe^{CNC}\cdot 2HBr$ (0.200 g, 0.500 mmol) was combined with 2 equiv of KO^tBu (0.120 g, 1.07 mmol) in 4 mL of THF forming a red/orange suspension and was left to stir for a few minutes. A portion of $[Cu(CH_3CN)_4](PF_6)$ (0.186 g, 0.500 mmol) in 1.0 mL of CH_3CN and 1.5 mL of THF was added, and the reaction mixture was left to stir for 16 h. The reaction mixture was then filtered through a glass frit to separate a yellow solid (A) from a yellow/orange filtrate (B). The solvent was removed from the filtrate B, and the resultant orange solid was triturated with THF, filtered, and dried under vacuum. The solid from the glass frit (A) was redissolved in CH_3CN forming a yellow suspension, which was filtered to remove a light yellow solid, presumably KBr. Complete solvent removal from the filtrate A afforded an intense yellow solid, which got combined with the solid obtained earlier from the first filtrate B providing an overall 65% yield (0.150 g). The attempts to grow suitable crystals for X-ray crystallography from CH_3CN were not successful due to the moderate solubility of the complex. ^1H NMR (CD_3CN with 0.05% v/v TMS, 400 MHz): δ = 8.35 (t, 1H; *p*-C_5H_3N, $^3J_{HH}$ = 8.0 Hz), 7.80 (d, 2H; $HCCH^{NHC}$, $^3J_{HH}$ = 2.0 Hz), 7.77 (d, 2H; *m*-C_5H_3N, $^3J_{HH}$ = 8.0 Hz), 7.18 (d, 2H; $HCCH^{NHC}$, $^3J_{HH}$ = 2.0 Hz), 3.27 ppm (s, 6H; CH_3). $^{13}C\{^1H\}$ NMR (CD_3CN with 0.05% v/v TMS, 101 MHz): δ 182.14, 149.80, 145.07, 125.22, 119.14, 114.15, 38.98 ppm. Elemental analysis (%) calcd for $C_{26}H_{26}Cu_2F_{12}N_{10}P_2$: C, 34.87; H, 2.93; N, 15.64. Found: C, 34.51; H, 2.95; N, 15.30.

$[Cu_2(IEt^{CNC})_2](PF_6)_2\cdot CH_3CN$, ***2**·CH$_3$CN*. A portion of $IEt^{CNC}\cdot 2HBr$ (0.200 g, 0.435 mmol) was combined with 2 equiv of KO^tBu (0.099 g, 0.882 mmol) in 5 mL of THF forming a red/brown suspension and was left to stir for a few minutes. A 2 mL solution of $[Cu(CH_3CN)_4](PF_6)$ (0.162 g, 0.435 mmol) in CH_3CN/THF (1:1) was added, and the reaction mixture was left to stir for 45 h. The reaction mixture was then filtered through a glass frit to separate a yellow solid from a light green filtrate. The solid was redissolved in 5 mL of CH_3CN forming a yellow suspension, which was filtered to remove a white solid, presumably KBr. The solvent was removed in vacuo from the filtrate giving an intense yellow solid in 66% yield (0.142 g). Yellow crystals of X-ray quality were grown by slow diffusion of ether into a solution of complex in acetonitrile. ^1H NMR (CD_3CN with 0.05% v/v TMS, 400 MHz): δ = 8.37 (t, 1H; *p*-C_5H_3N, $^3J_{HH}$ = 8.0 Hz), 7.85 (d, 2H; $HCCH^{NHC}$, $^3J_{HH}$ = 2.1 Hz), 7.81 (d, 2H; *m*-C_5H_3N, $^3J_{HH}$ = 8.0 Hz), 7.28 (d, 2H; $HCCH^{NHC}$, $^3J_{HH}$ = 2.0 Hz), 3.69 (q, 4H; CH_2CH_3, $^3J_{HH}$ = 7.3 Hz), 0.98 ppm (t, 6H; CH_2CH_3, $^3J_{HH}$ = 7.3 Hz). $^{13}C\{^1H\}$ NMR (CD_3CN with 0.05% v/v TMS, 101 MHz): δ 180.28, 149.92, 145.02, 123.76, 119.24, 114.12 (s, *m*-C_5H_3N), 47.63, 16.30 ppm. Elemental analysis (%) calcd for $C_{32}H_{37}Cu_2F_{12}N_{11}P_2$: C, 38.72; H, 3.76; N, 15.52. Found: C, 39.10; H, 3.77; N, 15.13.

$[Cu_2(IEt^{CNC})_2](BArF)_2\cdot C_4H_8O\cdot CH_3CN$, ***2**·C$_4H_8$O·CH$_3$CN*. This complex was prepared for electrochemical studies due to the good solubility in medium-polar solvents. A portion of $IEt^{CNC}\cdot 2HBr$ (0.100 g, 0.217 mmol) was combined with 2 equiv of KO^tBu (0.050 g, 0.446 mmol) in 2 mL of THF forming a light yellow suspension and was left to stir for a few minutes. A 2 mL solution of $[Cu(CH_3CN)_4]BArF$ (0.195 g, 0.217 mmol) in THF was added, and the reaction mixture was left to stir for 16 h. The reaction mixture was then filtered through Celite, and the solvent was removed in vacuo giving an intense yellow oil. The oil was dissolved in THF and precipitated with hexane as a yellow powder. The solid was filtered through a glass frit and dried under vacuum to provide a yellow powder in 54% yield (0.125 g). ^1H NMR (CD_3CN with 0.05% v/v TMS, 400 MHz): δ = 8.33 (t, 1H; *p*-C_5H_3N, $^3J_{HH}$ = 7.9 Hz), 7.78 (s, 2H; $HCCH^{NHC}$), 7.74 (d, 2H; *m*-C_5H_3N, $^3J_{HH}$ = 7.9 Hz), 7.23 (d, 2H; $HCCH^{NHC}$), 3.65 (q, 4H; CH_2CH_3, $^3J_{HH}$ = 6.9 Hz), 0.94 ppm (t, 6H; CH_2CH_3, $^3J_{HH}$ = 7.0 Hz). $^{13}C\{^1H\}$ NMR (CD_3CN with 0.05% v/v TMS, 101 MHz): δ 180.28, 149.92, 145.02, 123.76, 119.24, 114.12 (s, *m*-C_5H_3N), 47.63, 16.30 ppm. Elemental analysis (%) calcd for $C_{84}H_{45}B_2Cu_2F_{40}N_{11}O$: C, 47.30; H, 2.13; N, 7.22. Found: C, 47.29; H, 2.16; N, 7.01.

$[Cu_2(^iPr^{CNC})_2](PF_6)_2$, ***3***. A solution of KO^tBu (0.072 g, 0.643 mmol) in 2 mL of THF was added to $I^iPr^{CNC}\cdot 2HBr$ (0.150 g, 0.322 mmol) in THF (2 mL) forming a bright orange slurry, which was left to stir for a few minutes. A portion of $[Cu(CH_3CN)_4](PF_6)$ (0.120 g, 0.322

DOI: 10.1021/acs.inorgchem.6b01646
Inorg. Chem. XXXX, XXX, XXX−XXX

mmol) in 3 mL of CH_3CN/THF (1:1) was added, and the reaction mixture was left to stir for 21 h. The reaction mixture was filtered through a glass frit to separate a pale yellow solid from an intense yellow solution (first filtrate). The pale yellow solid was redissolved in acetonitrile and filtered to remove an off-white solid, presumably KBr. The solvent was removed in vacuo from the filtrate forming an intense yellow solid, which got combined with another portion of the solid collected after solvent removal from the first filtrate. The solid was recrystallized from a solution of acetonitrile layered with ether (0.142 g, 72% yield). The crystals obtained from slow diffusion of ether into acetonitrile were not suitable for X-ray crystallography. ^{1}H NMR (CD_3CN with 0.05% v/v TMS, 400 MHz): δ = 8.33 (t, 1H; *p*-C_5H_3N, $^3J_{HH}$ = 8.0 Hz), 7.82 (d, 2H; $HCCH^{NHC}$, $^3J_{HH}$ = 2.1 Hz), 7.74 (d, 2H; *m*-C_5H_3N, $^3J_{HH}$ = 8.1 Hz), 7.29 (d, 2H; $HCCH^{NHC}$, $^3J_{HH}$ = 2.1 Hz), 4.12 (br septet, 2H; $CH(CH_3)_2$), 1.07 ppm (broad d, 12H; $CH(CH_3)_2$). $^{13}C\{^1H\}$ NMR (CD_3CN with 0.05% v/v TMS, 101 MHz): δ 178.58, 149.94, 145.06, 121.69, 119.21, 113.94, 55.24, 23.29 ppm. Elemental analysis (%) calcd for $C_{34}H_{42}Cu_2F_{12}N_{10}P_2$: C, 40.52; H, 4.20; N, 13.90. Found: C, 40.56; H, 4.24; N, 13.85.

[Cu_2(I^iPr^{CNC})$_2$](SbF_6)$_2$, ***3-SbF$_6$***. This complex was prepared with a larger anion than PF_6 to improve the quality of crystals for X-ray analysis. A portion of I^iPr^{CNC}·2HBr (0.150 g, 0.322 mmol) was combined with 2 equiv of KO^{t}Bu (0.072 g, 0.643 mmol) in 6 mL of THF affording a bright red suspension, which was left to stir for a few minutes. A portion of [Cu(CH_3CN)$_4$](SbF_6) (0.149 g, 0.322 mmol) in 2 mL of CH_3CN/THF (1:1) was added,and the reaction mixture was left to stir for 18 h. The reaction mixture was filtered via a glass frit to separate an off-white solid from an intense yellow solution (first filtrate). The off-white solid was redissolved in CH_3CN and filtered to remove a white solid, presumably KBr from a yellow solution. The solution was combined with the first filtrate and concentrated under vacuum before layering with diethyl ether. The yield of recrystallized solid was 0.096 g (50%). Orange/yellow crystals suitable for X-ray crystallography were grown by ether diffusion into acetonitrile. ^{1}H NMR (CD_3CN with 0.05% v/v TMS, 400 MHz): δ = 8.34 (t, 1H; *p*-C_5H_3N, $^3J_{HH}$ = 8.1 Hz), 7.85 (d, 2H; $HCCH^{NHC}$, $^3J_{HH}$ = 2.1 Hz), 7.77 (d, 2H; *m*-C_5H_3N, $^3J_{HH}$ = 8.1 Hz), 7.30 (d, 2H; $HCCH^{NHC}$, $^3J_{HH}$ = 2.1 Hz), 4.11 (septet, 2H; $CH(CH_3)_2$, $^3J_{HH}$ = 6.7 Hz), 1.04 ppm (d, 12H; $CH(CH_3)_2$, $^3J_{HH}$ = 6.7 Hz). $^{13}C\{^1H\}$ NMR (CD_3CN with 0.05% v/v TMS, 101 MHz): δ 178.62, 149.96, 145.06, 121.70, 119.29, 114.01, 55.22, 23.29 ppm. Elemental analysis (%) calcd for $C_{42}H_{54}Cu_2F_{12}N_{14}Sb_2$: C, 37.27; H, 4.02; N, 14.49. Found: C, 37.32; H, 3.94; N, 12.81.

[Cu_2($IMe^{C^N^C}$)$_2$](PF_6)$_2$, ***4***. A solution of KO^{t}Bu (0.078 g, 0.700 mmol) in 2 mL of THF was added to $IMe^{C^N^C}$·2HBr (0.150 g, 0.349 mmol) in THF (2 mL) forming a yellow/orange slurry, which was left to stir for a few minutes. A portion of [Cu(CH_3CN)$_4$](PF_6) (0.130 g, 0.349 mmol) in 1.0 mL of CH_3CN and 1.5 mL of THF was added, and the reaction mixture was left to stir for 21 h. The reaction mixture was then filtered to separate a yellow solid from a pale yellow filtrate. The solid was suspended in CH_3CN forming a yellow solution and an off-white solid (KBr), which was filtered off via a glass frit. The solvent was removed in vacuo from the filtrate leading to a yellow solid in 40% yield (0.066 g). X-ray quality crystals were grown by vapor diffusion of ether into acetonitrile. ^{1}H NMR (CD_3CN with 0.05% v/v TMS, 400 MHz): δ = 7.91 (t, 1H; *p*-C_5H_3N, $^3J_{HH}$ = 7.7 Hz), 7.54 (d, 2H; *m*-C_5H_3N, $^3J_{HH}$ = 7.8 Hz), 7.24 (d, 2H; $HCCH^{NHC}$, $^3J_{HH}$ = 1.8 Hz), 7.12 (d, 2H; $HCCH^{NHC}$, $^3J_{HH}$ = 1.8 Hz), 5.24 (s, 4H; CH_2), 3.85 ppm (s, 6H; CH_3). $^{13}C\{^1H\}$ NMR (CD_3CN with 0.05% v/v TMS, 101 MHz): δ 179.84, 155.83, 140.87, 125.12, 123.55, 122.20, 55.26, 39.43 ppm. Elemental analysis (%) calcd for $C_{30}H_{38}Cu_2F_{12}N_{10}P_2$: C, 37.70; H, 4.01; N, 14.66. Found: C, 28.52; H, 2.65; N, 11.05. The CHN analyses are an average of two replicate runs. The data is consistent with an oxidized complex with the proposed chemical formula $C_{15}H_{20}CuF_{12}N_5OP_2$. The calculated C, H, and N for this compound are (%) C, 28.16; H, 3.15; N, 10.95.

[Cu($IEt^{C^N^C}$)]PF_6, ***5***. A portion of $IEt^{C^N^C}$·2HBr (0.200 g, 0.437 mmol) was combined with 2 equiv of KO^{t}Bu (0.098 g, 0.879 mmol) in 5 mL of THF forming a yellow suspension and was left to stir for a few minutes. A 2 mL solution of [Cu(CH_3CN)$_4$](PF_6) (0.163 g, 0.437 mmol) in CH_3CN/THF (1:1) was added, and the reaction mixture was left to stir for 20 h. The reaction mixture was then filtered through a glass frit to separate an off-white solid from a yellow filtrate. The solid was redissolved in 5 mL of CH_3CN forming a yellow suspension, which was filtered to remove a white solid (KBr). The solvent was then removed in vacuo from the solution to give a yellow solid (portion A). The filtrate of the reaction mixture was also kept under vacuum for solvent removal leading to a yellow solid, which was triturated with 10−15 mL of THF (portion B). A recrystallization of the yellow solid from both portions, A and B, in CH_3CN/Et_2O afforded X-ray quality cubic crystals in 68% yield (0.150 g). ^{1}H NMR (CD_3CN with 0.05% v/v TMS, 400 MHz): δ = 7.92 (t, 1H; *p*-C_5H_3N, $^3J_{HH}$ = 7.8 Hz), 7.55 (d, 2H; *m*-C_5H_3N, $^3J_{HH}$ = 7.7 Hz), 7.25 (d, 2H; $HCCH^{NHC}$, $^3J_{HH}$ = 1.8 Hz), 7.19 (d, 2H; $HCCH^{NHC}$, $^3J_{HH}$ = 1.8 Hz), 5.26 (s, 4H; CH_2), 4.21 (q, 4H; CH_2CH_3, $^3J_{HH}$ = 7.3 Hz), 1.41 ppm (t, 6H; CH_2CH_3, $^3J_{HH}$ = 7.3 Hz). $^{13}C\{^1H\}$ NMR (CD_3CN with 0.05% v/v TMS, 101 MHz): δ 179.08, 155.76, 140.86, 125.09, 123.61, 120.04, 55.18, 47.89, 17.49 ppm. Elemental analysis (%) calcd for $C_{34}H_{46}Cu_2F_{12}N_{10}P_2$: C, 40.36; H, 4.58; N, 13.84. Found: C, 40.48; H, 4.30; N, 13.84.

[Cu_2($I^iPr^{C^N^C}$)$_2$](PF_6)$_2$, ***6***. A portion of $I^iPr^{C^N^C}$·2HBr (0.171 g, 0.352 mmol) was combined with 2 equiv of KO^{t}Bu (0.078 g, 0.698 mmol) in 5 mL of THF forming a yellow/orange suspension and was left to stir for a few minutes. A portion of [Cu(CH_3CN)$_4$](PF_6) (0.130 g, 0.349 mmol) in 2 mL of CH_3CN/THF (1:1) was added, and the reaction mixture was left to stir for 21 h. The reaction mixture was then filtered through a glass frit to separate an off-white solid (KBr) from a yellow filtrate. The solvent was removed from the filtrate in vacuo leading to a shiny yellow solid, which was recrystallized from CH_3CN/Et_2O in 68% yield (0.126 g). Yellow crystals suitable for X-ray crystallography were grown by vapor diffusion of Et_2O into CH_3CN. ^{1}H NMR (CD_3CN with 0.05% v/v TMS, 400 MHz): δ = 7.92 (t, 1H; *p*-C_5H_3N, $^3J_{HH}$ = 7.7 Hz), 7.55 (d, 2H; *m*-C_5H_3N, $^3J_{HH}$ = 7.7 Hz), 7.27 (d, 2H; $HCCH^{NHC}$, $^3J_{HH}$ = 1.8 Hz), 7.22 (d, 2H; $HCCH^{NHC}$, $^3J_{HH}$ = 1.8 Hz), 5.26 (s, 4H; CH_2), 4.80 (septet, 2H; $CH(CH_3)_2$, $^3J_{HH}$ = 6.8 Hz), 1.48 ppm (d, 12H; $CH(CH_3)_2$, $^3J_{HH}$ = 6.8 Hz). $^{13}C\{^1H\}$ NMR (CD_3CN with 0.05% v/v TMS, 101 MHz): δ 178.58, 155.53, 140.83, 124.94, 123.72, 117.53, 55.19, 55.06, 23.88 ppm. Elemental analysis (%) calcd for $C_{38}H_{54}Cu_2F_{12}N_{10}P_2$: C, 42.74; H, 5.10; N, 13.12. Found: C, 42.67; H, 4.83; N, 12.86.

Electrochemistry. Cyclic and differential pulse voltammetry studies of complexes **1**−**6** and IMe^{CNC}·2HPF$_6$ were performed in CH_3CN using a 5 mM concentration of each compound and 0.1 M ^{n}Bu$_4$PF$_6$ (tetra-*n*-butylammonium hexafluorophosphate) as the supporting electrolyte under an inert atmosphere. The electrochemistry experiment setup consisted of a three-electrode cell connected to an external CHI 730C potentiostat run by a personal computer with CHI software. A glassy carbon electrode (0.5 mm diameter) was employed as the working electrode, with Ag/$AgNO_3$ (0.01 M) as the reference and Pt wire as the counter electrode. The working electrode was cleaned between experiments using a polishing pad and carefully dried. All potentials are reported versus [Fe(C_5H_5)$_2$]$^+$/[Fe(C_5H_5)$_2$] by subtracting 0.143 V from the measured value versus Ag/$AgNO_3$ electrode.

CONCLUSIONS

The single-step syntheses of six new Cu(I) complexes with two groups of pincer pyridine-based N-heterocyclic carbene ligands, $I(R)^{CNC}$ and $I(R)^{C^N^C}$, are reported herein with the full structural, spectroscopic, solution conductivity, and electrochemical characterization. These compounds complement and fill in the void of structurally well-characterized Cu(I)−$I(R)^{CNC}$ and Cu(I)−$I(R)^{C^N^C}$ complexes with small wingtip substituents (R = Me, Et, and ^{i}Pr) in literature. All the copper complexes present cuprophilic interactions in solid state, except Cu−$IEt^{C^N^C}$ in which the syn orientation of Et groups prevents the Cu ions' contact. The less flexible structure of $I(R)^{CNC}$ ligands as well as their helical coordination modes

DOI: 10.1021/acs.inorgchem.6b01646
Inorg. Chem. XXXX, XXX, XXX−XXX

maintains the integrity of binuclear complexes in both solid and solution state. In contrast, the more flexible I(R)$^{C^N^C}$ with all three donor sites of a pincer ligand bound to one copper allow the adjacent metals' contact only in the solid state but at a shorter Cu···Cu distance than those of Cu−I(R)^{CNC} complexes.

The two classes of pincer NHC ligands are capable of accommodating different valences of copper to varying extents. The Cu−I(R)^{CNC} complexes undergo multiple speciation in coordinating solvents forming mono- and binuclear complexes that are oxidized by one-electron under electrochemical conditions. The unique reversible Cu(II)/Cu(I) redox couples in Cu−I(R)$^{C^N^C}$ at close potentials to that of tripodal NHC systems, however, demonstrate the ability of simple pincer CNC ligands to stabilize both low and high oxidation states of copper. The work is currently in progress to examine the syntheses of Cu(II)−I(R)^{CNC} and Cu(II)−I(R)$^{C^N^C}$ complexes under chemical conditions.

■ ASSOCIATED CONTENT

Supporting Information

The Supporting Information is available free of charge on the ACS Publications website at DOI: 10.1021/acs.inorgchem.6b01646.

Crystallographic data collection table, ^{1}H and ^{13}C{^{1}H} NMR spectra for **1**-**6** and imidazolium salts, ORTEP diagram of **2** with long-distance interactions, CV of complexes **1**-**6** with varying potentials, and scan rates (PDF)

Crystallographic information file for **5** (CIF)

Crystallographic information file for **2** (CIF)

Crystallographic information file for **3**-SbF_6 (CIF)

Crystallographic information file for **6** (CIF)

Crystallographic information file for **4** (CIF)

■ AUTHOR INFORMATION

Corresponding Author

*E-mail: tahsini@okstate.edu. Phone: +1 (405) 744 4370. Fax: (405) 744-6007.

Notes

The authors declare no competing financial interest.

■ ACKNOWLEDGMENTS

We gratefully acknowledge Oklahoma State University start-up funding (L.T.), NSF-BIR 9512269, the Oklahoma State Regents for Higher Education, the W. M. Keck Foundation, and Conoco Inc. (NMR Spectrometers in the research facility center at Oklahoma State) and the OSU fund (Single Crystal X-ray Diffraction in the OSU core facility center) for financial support.

■ REFERENCES

(1) Arduengo, A. J.; Harlow, R. L.; Kline, M. A Stable Crystalline Carbene. *J. Am. Chem. Soc.* **1991**, *113*, 361−363.

(2) Herrmann, W. A.; Elison, M.; Fischer, J.; Köcher, C.; Artus, G. R. J. Metal Complexes of N-Heterocyclic Carbenes—a New Structural Principle for Catalysts in Homogeneous Catalysis. *Angew. Chem., Int. Ed. Engl.* **1995**, *34*, 2371−2374.

(3) Samojłowicz, C.; Bieniek, M.; Grela, K. Ruthenium-Based Olefin Metathesis Catalysts Bearing N-Heterocyclic Carbene Ligands. *Chem. Rev.* **2009**, *109*, 3708−3742.

(4) Vougioukalakis, G. C.; Grubbs, R. H. Ruthenium-Based Heterocyclic Carbene-Coordinated Olefin Metathesis Catalysts. *Chem. Rev.* **2010**, *110*, 1746−1787.

(5) Valente, C.; Calimsiz, S.; Hoi, K. H.; Mallik, D.; Sayah, M.; Organ, M. G. The Development of Bulky Palladium NHC Complexes for the Most-Challenging Cross-Coupling Reactions. *Angew. Chem., Int. Ed.* **2012**, *51*, 3314−3332.

(6) Lazreg, F.; Nahra, F.; Cazin, C. S. J. Copper−NHC Complexes in Catalysis. *Coord. Chem. Rev.* **2015**, *293*−*294*, 48−79.

(7) Gaillard, S.; Cazin, C. S. J.; Nolan, S. P. N-Heterocyclic Carbene Gold(I) and Copper(I) Complexes in C−H Bond Activation. *Acc. Chem. Res.* **2012**, *45*, 778−787.

(8) Lin, J. C. Y.; Huang, R. T. W.; Lee, C. S.; Bhattacharyya, A.; Hwang, W. S.; Lin, I. J. B. Coinage Metal−N-Heterocyclic Carbene Complexes. *Chem. Rev.* **2009**, *109*, 3561−3598.

(9) Arnold, P. L. Organometallic Chemistry of Silver and Copper N-Heterocyclic Carbene Complexes. *Heteroat. Chem.* **2002**, *13*, 534−539.

(10) Diez-Gonzalez, S.; Escudero-Adan, E. C.; Benet-Buchholz, J.; Stevens, E. D.; Slawin, A. M. Z.; Nolan, S. P. [(NHC)CuX] Complexes: Synthesis, Characterization and Catalytic Activities in Reduction Reactions and Click Chemistry. On the Advantage of Using Well-Defined Catalytic Systems. *Dalton Trans.* **2010**, *39*, 7595−7606.

(11) Citadelle, C. A.; Nouy, E. L.; Bisaro, F.; Slawin, A. M. Z.; Cazin, C. S. J. Simple and Versatile Synthesis of Copper and Silver N-Heterocyclic Carbene Complexes in Water or Organic Solvents. *Dalton Trans.* **2010**, *39*, 4489−4491.

(12) Mankad, N. P.; Laitar, D. S.; Sadighi, J. P. Synthesis, Structure, and Alkyne Reactivity of a Dimeric (Carbene)Copper(I) Hydride. *Organometallics* **2004**, *23*, 3369−3371.

(13) Chun, J.; Lee, H. S.; Jung, I. G.; Lee, S. W.; Kim, H. J.; Son, S. U. Cu_2o: A Versatile Reagent for Base-Free Direct Synthesis of NHC-Copper Complexes and Decoration of 3d-MOF with Coordinatively Unsaturated NHC-Copper Species. *Organometallics* **2010**, *29*, 1518−1521.

(14) Landers, B.; Navarro, O. Microwave-Assisted Synthesis of (N-Heterocyclic Carbene)MCl Complexes of Group 11 Metals. *Eur. J. Inorg. Chem.* **2012**, *2012*, 2980−2982.

(15) Diez-Gonzalez, S.; Nolan, S. P. [$(NHC)_2$Cu]X Complexes as Efficient Catalysts for Azide-Alkyne Click Chemistry at Low Catalyst Loadings. *Angew. Chem., Int. Ed.* **2008**, *47*, 8881−8884.

(16) Lazreg, F.; Slawin, A. M. Z.; Cazin, C. S. J. Heteroleptic Bis(N-Heterocyclic Carbene)Copper(I) Complexes: Highly Efficient Systems for the [3 + 2] Cycloaddition of Azides and Alkynes. *Organometallics* **2012**, *31*, 7969−7975.

(17) Santoro, O.; Lazreg, F.; Cordes, D. B.; Slawin, A. M. Z.; Cazin, C. S. J. Homoleptic and Heteroleptic Bis- NHC Cu(I) Complexes as Carbene Transfer Reagents. *Dalton Trans.* **2016**, *45*, 4970−4973.

(18) Guo, S.; Lim, M. H.; Huynh, H. V. Copper(I) Heteroleptic Bis(NHC) and Mixed NHC/Phosphine Complexes: Syntheses and Catalytic Activities in the One-Pot Sequential CuAAC Reaction of Aromatic Amines. *Organometallics* **2013**, *32*, 7225−7233.

(19) Ibrahim, H.; Guillot, R.; Cisnetti, F.; Gautier, A. [{Cu(IPr)}$_2$(M-OH)[BF_4]: Synthesis and Halide-Free CuACC Catalysis. *Chem. Commun.* **2014**, *50*, 7154−7156.

(20) Zhang, L.; Cheng, J.; Hou, Z. Highly Efficient Catalytic Hydrosilylation of Carbon Dioxide by an N-Heterocyclic Carbene Copper Catalyst. *Chem. Commun.* **2013**, *49*, 4782−4784.

(21) Hohloch, S.; Scheiffele, D.; Sarkar, B. Activating Azides and Alkynes for the Click Reaction with [Cu(ANHC)$_2$I] or [Cu(ANHC)$_2$]$^+$ (ANHC = Triazole-Derived Abnormal Carbenes): Structural Characterization and Catalytic Properties. *Eur. J. Inorg. Chem.* **2013**, *2013*, 3956−3965.

(22) Laitar, D. S.; Tsui, E. Y.; Sadighi, J. P. Copper(I) B-Boroalkyls from Alkene Insertion: Isolation and Rearrangement. *Organometallics* **2006**, *25*, 2405−2408.

(23) Lillo, V.; Fructos, M. R.; Ramírez, J.; Braga, A. A. C.; Maseras, F.; Díaz-Requejo, M. M.; Pérez, P. J.; Fernández, E. A Valuable, Inexpensive Cu^{I}/N-Heterocyclic Carbene Catalyst for the Selective Diboration of Styrene. *Chem. - Eur. J.* **2007**, *13*, 2614−2621.

(24) Lee, Y.; Hoveyda, A. H. Efficient Boron−Copper Additions to Aryl-Substituted Alkenes Promoted by NHC−Based Catalysts.

DOI: 10.1021/acs.inorgchem.6b01646
Inorg. Chem. XXXX, XXX, XXX−XXX

Enantioselective Cu-Catalyzed Hydroboration Reactions. *J. Am. Chem. Soc.* **2009**, *131*, 3160−3161.
(25) Poyatos, M.; Mata, J. A.; Peris, E. Complexes with Poly(N-Heterocyclic Carbene) Ligands: Structural Features and Catalytic Applications. *Chem. Rev.* **2009**, *109*, 3677−3707.
(26) Hu, X.; Castro-Rodriguez, I.; Meyer, K. A Bis-Carbenealkenyl Copper(I) Complex from a Tripodal Tris-Carbene Ligand. *Organometallics* **2003**, *22*, 3016−3018.
(27) Hu, X.; Castro-Rodriguez, I.; Meyer, K. Copper Complexes of Nitrogen-Anchored Tripodal N-Heterocyclic Carbene Ligands. *J. Am. Chem. Soc.* **2003**, *125*, 12237−12245.
(28) Wan, X.-J.; Xu, F.-B.; Li, Q.-S.; Song, H.-B.; Zhang, Z.-Z. Synthesis and Crystal Structure of Metal (M = Ag, Cu) Crown Ether with N-Heterocyclic Carbene Linkage. *Inorg. Chem. Commun.* **2005**, *8*, 1053−1055.
(29) Arnold, P. L.; Scarisbrick, A. C.; Blake, A. J.; Wilson, C. Chelating Alkoxy-N-Heterocyclic Carbene Complexes of Silver and Copper. *Chem. Commun.* **2001**, 2340−2341.
(30) Shishkov, I. V.; Rominger, F.; Hofmann, P. Reversible Substrate Binding at Copper Centers in Neutral Copper(I) Carbene Complexes Derived from Bis(3-Tert-Butylimidazole-2-Ylidene)Methane. *Dalton Trans.* **2009**, 1428−1435.
(31) Liu, B.; Xia, Q.; Chen, W. Direct Synthesis of Iron, Cobalt, Nickel, and Copper Complexes of N-Heterocyclic Carbenes by Using Commercially Available Metal Powders. *Angew. Chem., Int. Ed.* **2009**, *48*, 5513−5516.
(32) Zhong, R.; Pöthig, A.; Mayer, D. C.; Jandl, C.; Altmann, P. J.; Herrmann, W. A.; Kühn, F. E. Spectroscopic and Structural Properties of Bridge-Functionalized Dinuclear Coinage-Metal (Cu, Ag, and Au) NHC Complexes: A Comparative Study. *Organometallics* **2015**, *34*, 2573−2579.
(33) Sathyanarayana, A.; Metla, B. P. R.; Sampath, N.; Prabusankar, G. Dinuclear, Tetranuclear and Polynuclear Copper(I)-Ethylene-Bridged Bis-N-Heterocyclic Carbene Complexes. *J. Organomet. Chem.* **2014**, *772*−*773*, 210−216.
(34) Fierro-Gonzalez, J. C.; Gates, B. C. Catalysis by Gold Dispersed on Supports: The Importance of Cationic Gold. *Chem. Soc. Rev.* **2008**, *37*, 2127−2134.
(35) Grundner, S.; Markovits, M. A. C.; Li, G.; Tromp, M.; Pidko, E. A.; Hensen, E. J. M.; Jentys, A.; Sanchez-Sanchez, M.; Lercher, J. A. Single-Site Trinuclear Copper Oxygen Clusters in Mordenite for Selective Conversion of Methane to Methanol. *Nat. Commun.* **2015**, *6*, 7546.
(36) Oms, O.; Yang, S.; Salomon, W.; Marrot, J.; Dolbecq, A.; Rivière, E.; Bonnefont, A.; Ruhlmann, L.; Mialane, P. Heteroanionic Materials Based on Copper Clusters, Bisphosphonates, and Polyoxometalates: Magnetic Properties and Comparative Electrocatalytic No_x Reduction Studies. *Inorg. Chem.* **2016**, *55*, 1551−1561.
(37) Riener, K.; Pothig, A.; Cokoja, M.; Herrmann, W. A.; Kuhn, F. E. Structure and Spectroscopic Properties of the Dimeric Copper(I) N-Heterocyclic Carbene Complex $[Cu_2(CNC_{t\text{-}Bu})_2](PF_6)_2$. *Acta Crystallogr., Sect. C: Struct. Chem.* **2015**, *71*, 643−646.
(38) Liu, B.; Ma, X.; Wu, F.; Chen, W. Simple Synthesis of Neutral and Cationic Cu-NHC Complexes. *Dalton Trans.* **2015**, *44*, 1836−1844.
(39) Pell, T. P.; Wilson, D. J. D.; Skelton, B. W.; Dutton, J. L.; Barnard, P. J. Heterobimetallic N-Heterocyclic Carbene Complexes: A Synthetic, Spectroscopic, and Theoretical Study. *Inorg. Chem.* **2016**, *55*, 6882−6891.
(40) Lake, B. R. M.; Willans, C. E. Remarkable Stability of Copper(II)−N-Heterocyclic Carbene Complexes Void of an Anionic Tether. *Organometallics* **2014**, *33*, 2027−2038.
(41) Saitoh, M.; Balch, A. L.; Yuasa, J.; Kawai, T. Effects of Counter Anions on Intense Photoluminescence of 1-D Chain Gold(I) Complexes. *Inorg. Chem.* **2010**, *49*, 7129−7134.
(42) Matsumoto, K.; Matsumoto, N.; Ishii, A.; Tsukuda, T.; Hasegawa, M.; Tsubomura, T. Structural and Spectroscopic Properties of a Copper(I)-Bis(N-Heterocyclic)Carbene Complex. *Dalton Trans.* **2009**, 6795−6801.
(43) Liu, B.; Chen, C.; Zhang, Y.; Liu, X.; Chen, W. Dinuclear Copper(I) Complexes of Phenanthrolinyl-Functionalized NHC Ligands. *Organometallics* **2013**, *32*, 5451−5460.
(44) Geary, W. J. The Use of Conductivity Measurements in Organic Solvents for the Characterisation of Coordination Compounds. *Coord. Chem. Rev.* **1971**, *7*, 81−122.
(45) Feltham, R. D.; Hayter, R. G. 875. The Electrolyte Type of Ionized Complexes. *J. Chem. Soc.* **1964**, 4587−4591.
(46) Delahay, P. Theory of Irreversible Waves in Oscillographic Polarography. *J. Am. Chem. Soc.* **1953**, *75*, 1190−1196.
(47) Brad, A. J.; Faulkner, L. R. *Electrochemical Methods: Fundamentals and Applications*; John Wiley and Sons, Inc.: New York, 2001.
(48) Eggleston, M. K.; McMillin, D. R.; Koenig, K. S.; Pallenberg, A. J. Steric Effects in the Ground and Excited States of $Cu(NN)_2^+$ Systems. *Inorg. Chem.* **1997**, *36*, 172−176.
(49) James, B. R.; Williams, R. J. P. 383. The Oxidation-Reduction Potentials of Some Copper Complexes. *J. Chem. Soc.* **1961**, *0*, 2007−2019.
(50) Hawkins, C. J.; Perrin, D. D. 553. Oxidation-Reduction Potentials of Metal Complexes in Water. Part II. Copper Complexes with 2,9-Dimethyl- and 2-Chloro-1,10-Phenanthroline. *J. Chem. Soc.* **1963**, *0*, 2996−3002.
(51) Kubas, G. J. Tetrakis(Acetonitrile)Copper(1+) Hexafluorophosphate(−1). *Inorg. Synth.* **1990**, *28*, 68−70.
(52) Peris, E.; Loch, J. A.; Mata, J.; Crabtree, R. H. A Pd Complex of a Tridentate Pincer Cnc Bis-Carbene Ligand as a Robust Homogenous Heck Catalyst. *Chem. Commun.* **2001**, 201−202.
(53) Serra, D.; Cao, P.; Cabrera, J.; Padilla, R.; Rominger, F.; Limbach, M. Development of Platinum(II) and -(IV) CNC Pincer Complexes and Their Application in a Hydrovinylation Reaction. *Organometallics* **2011**, *30*, 1885−1895.

DOI: 10.1021/acs.inorgchem.6b01646
Inorg. Chem. XXXX, XXX, XXX−XXX